Electronic supplementary information

The enhanced thermal stability for NIR emission $A_2InCl_5 \cdot H_2O:Cr^{3+}$ phosphor based on A site regulation

Lingkang Yu,[a,b] Yining Wang,[a,b] Xiaole Xing,[a,b] Zheng Xu,[a,b] Mengmeng Shang,[*a,b]

[a] Key Laboratory for Liquid-Solid Structural Evolution and Processing of Materials (Ministry of Education), School of Material Science and Engineering, Shandong University, Jinan 250061, P. R. China

[b]Shenzhen Research Institute of Shandong University, Shandong University, Shenzhen 518063, P. R. China

*Email: mmshang@sdu.edu.cn

Experimental section

Materials.

Cesium chloride (CsCl, Aladdin, 99.99%), Indium oxide (In_2O_3, Jining Tianyi New Materials Co.,Ltd, 99.99%), Chromium chloride ($CrCl_3$, Aladdin, 99.99%), Potassium carbonate (K_2CO_3, Sinopharm Chemical Reagent Co., Ltd, analytical pure), Rubidium carbonate (Rb_2CO_3, Aladdin, 99.8%), Sodium chloride (NaCl, Aladdin, 99.99%), Hydrochloric acid and ethanol were purchased from Sinopharm Chemical Reagent Co., Ltd. All materials were used without further purification.

Synthesis of $Cs_2InCl_5 \cdot H_2O$:xCr^{3+} powder.

Cr^{3+} doped $Cs_2InCl_5 \cdot H_2O$ crystal powders were prepared following a hydrothermal method. In detail, 2 mmol CsCl, x mmol $CrCl_3$ and (1-x)/2 mmol In_2O_3 were dissolved with 10 ml HCl in a 25 ml Teflon autoclave (x was set as 0, 0.05, 0.10, 0.15, 0.20, 0.25, 0.30, respectively). The solution was heated at 160 °C for 6 h, then slowly cooled to room temperature. The as-synthesized crystal powders were then filtered out and washed 2~3 times with ethanol, and finally dried in a furnace at 60 °C for overnight.

Synthesis of $(Cs_{1-y}Rb_y)_2InCl_5 \cdot H_2O$:0.25$Cr^{3+}$ powder.

0.25 mmol $CrCl_3$, 0.375 mmol In_2O_3, y mmol Rb_2CO_3 and (2-2y) mmol CsCl were dissolved with 10ml HCl in a 25ml Teflon autoclave (y was set as 0, 0.2, 0.4, 0.6, 0.8, 1.0, respectively). The solution was heated at 160 °C for 6 h, then slowly cooled to room temperature. The as-synthesized crystals were then filtered out and washed with ethanol 2~3 times, and finally dried in a furnace at 60 °C for overnight.

Synthesis of $(Cs_{1-z}K_z)_2InCl_5 \cdot H_2O$:0.25$Cr^{3+}$ powder.

$(Cs_{1-z}K_z)_2InCl_5 \cdot H_2O$:0.25$Cr^{3+}$ crystals were prepared with the similar procedures to that of $(Cs_{1-y}Rb_y)_2InCl_5 \cdot H_2O$:0.25$Cr^{3+}$ crystals above, except z was set as 0, 0.1, 0.2, 0.3, 0.4, 0.5, respectively.

Characterization.

The diffuse reflection spectra (DRS) were recorded on an UV−vis−NIR spectrophotometer (UV-3600 plus, Shimadzu, Japan). The composition and phase of materials were detected by powder X-ray diffraction (XRD) measurements using a D8 Focus diffractometer (Bruker) with Cu Kα radiation (λ = 0.15405 nm). The General Structure Analysis System II (GSAS II) program was used to conduct XRD refinements. The morphology and elemental composition were obtained by a field-emission scanning electron microscope (SU-70, Hitachi) equipped with an energy-dispersive spectrometer. The steady-state photoluminescence (PL) and photoluminescence excitation (PLE) spectra, the decay curves, temperature-dependent PL spectra (77-425K) and PLQYs were recorded via an Edinburgh fluorescence spectrometer (FLS 980) equipped with a continuous 450 W xenon lamp as the steady-state excitation sources, a pulsed high-energy Xenon flash lamp (μF_2) as the transient excitation source, and an integrating sphere.The thermogravimetric (TG) tests were detected by a thermogravimetric analyzer (TGA8000, PerkinElmer). The differential scanning calorimetry (DSC) curves were detected by Differential Scanning Calorimeter (DSC8000 PerkinElmer). The quantum efficiency for NIR emission of the as-prepared phosphors was recorded by vis–NIR absolute quantum efficiency test system (Hamamatsu C9920-02) equipped with 3.3-inch integrating sphere. In order to evaluate the Debye temperature of $Cs_2InCl_5{\cdot}H_2O{:}0.25Cr^{3+}$, $(Cs_{0.6}Rb_{0.4})_2InCl_5{\cdot}H_2O{:}0.25Cr^{3+}$ and $(Cs_{0.7}K_{0.3})_2InCl_5{\cdot}H_2O{:}0.25Cr^{3+}$, DFT method was used. The generalized gradient approximation with the Perdew-Burke-Ernzerhof functional was used as the exchange correlation potential. All calculations were performed using a 650 eV cut-off energy. In the Brillouin zone, a 2 × 3 × 4 k-mesh grid centered on gamma was used, and the self-consistent charge density was determined by the Monkhorst-Pack scheme. The lattice was completely relaxed until the atomic force was<−0.02 eV $Å^{-1}$.

Debye temperature ($\Theta_{D,i}$) was calculated according to the anisotropic atomic displacement parameter, using the following formula:

$$\Theta_{D,i} = \sqrt{\frac{3\hbar T N_A}{A_i k_B U_{iso,i}}} \qquad (eq.S1)$$

The formula incorporates the atomic weight of the atom (A_i), reduced Planck's constant ($\hbar$), Boltzmann's constant (k_B), the average atomic displacement parameter ($U_{iso,i}$). The $\Theta_{D,i}$, value is inversely proportional to $U_{iso,i}$.

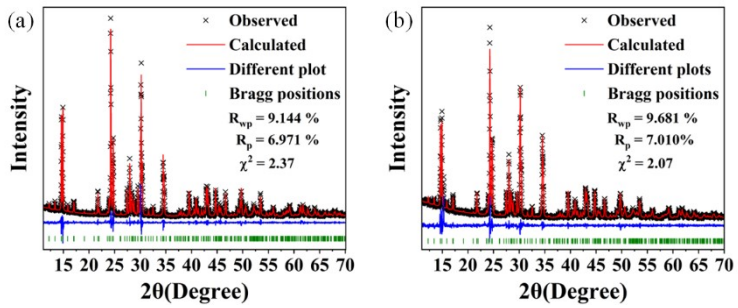

Fig. S1.a b) XRD Rietveld refinement of $Cs_2InCl_5 \cdot H_2O$ matrix and $Cs_2InCl_5 \cdot H_2O$:0.25Cr^{3+}.

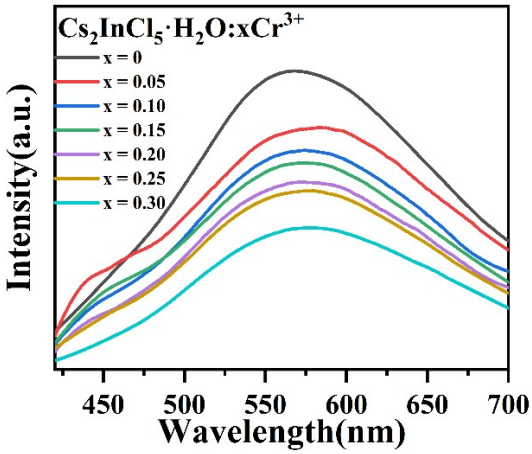

Fig.S2. PL spectra for the $Cs_2InCl_5 \cdot H_2O:xCr^{3+}$(x = 0 ~ 0.30) phosphors at 360 nm excitation wavelength.

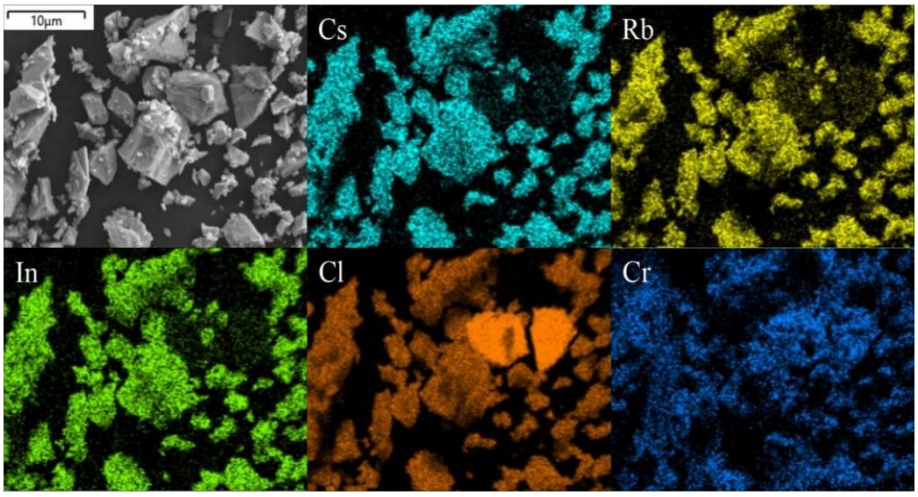

Fig. S3. SEM image and elemental mapping images of $(Cs_{0.6}Rb_{0.4})_2InCl_5 \cdot H_2O$:0.25$Cr^{3+}$.

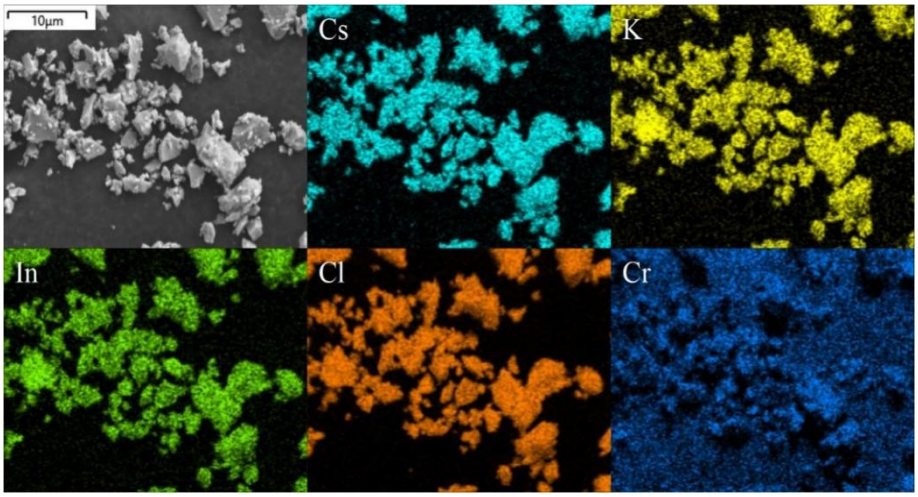

Fig. S4. SEM image and elemental mapping images of $(Cs_{0.7}K_{0.3})_2InCl_5 \cdot H_2O$:0.25$Cr^{3+}$.

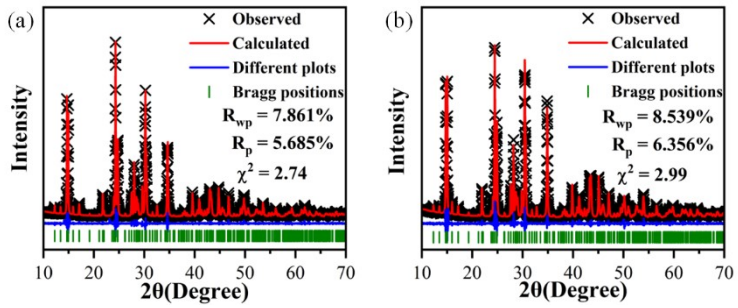

Fig. S5. a,b) XRD Rietveld refinement of $(Cs_{0.6}Rb_{0.4})_2InCl_5 \cdot H_2O{:}0.25Cr^{3+}$ and $(Cs_{0.7}K_{0.3})_2InCl_5 \cdot H_2O{:}0.25Cr^{3+}$.

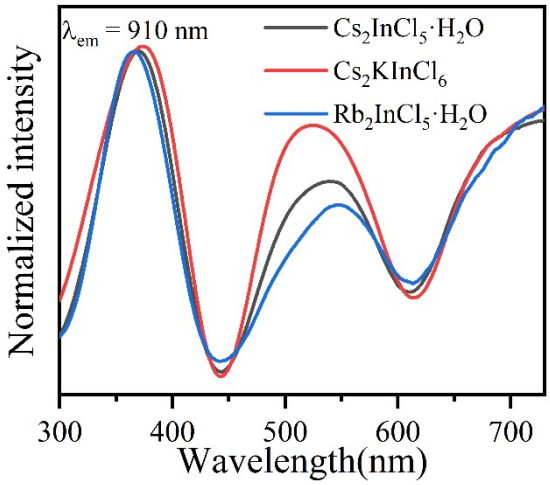

Fig. S6. PLE spectra of $Cs_2InCl_5 \cdot H_2O$:0.25Cr^{3+}, Cs_2KInCl_6:0.25Cr^{3+}, $Rb_2InCl_5 \cdot H_2O$:0.25Cr^{3+}.

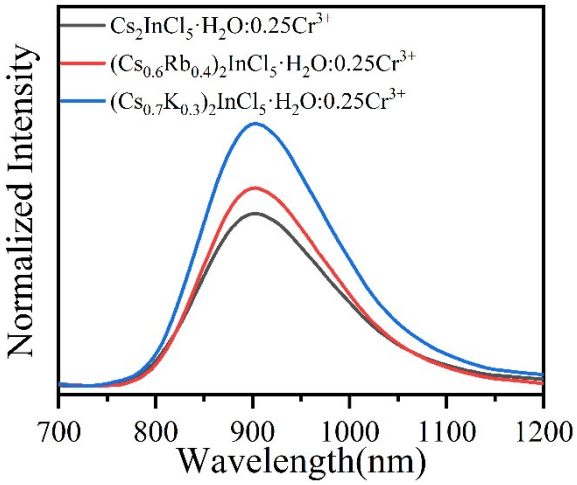

Fig. S7. Normalized PL spectrum of $Cs_2InCl_5 \cdot H_2O:0.25Cr^{3+}$, $(Cs_{0.6}Rb_{0.4})_2InCl_5 \cdot H_2O:0.25Cr^{3+}$ and $(Cs_{0.7}K_{0.3})_2InCl_5 \cdot H_2O:0.25Cr^{3+}$.

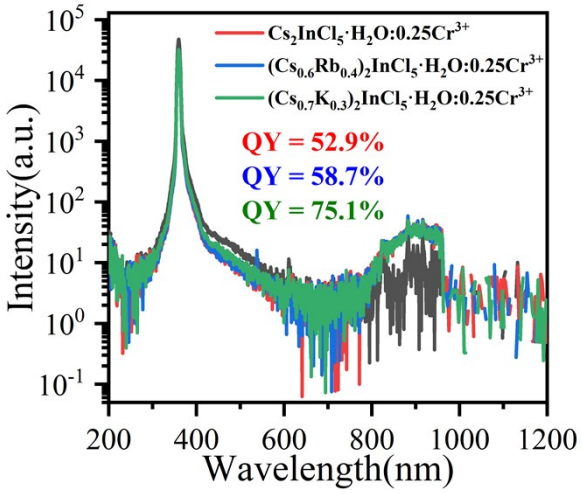

Fig. S8. PLQY of $Cs_2InCl_5 \cdot H_2O:0.25Cr^{3+}$, $(Cs_{0.6}Rb_{0.4})_2InCl_5 \cdot H_2O:0.25Cr^{3+}$ and $(Cs_{0.7}K_{0.3})_2InCl_5 \cdot H_2O:0.25Cr^{3+}$ under 360 nm excitation.

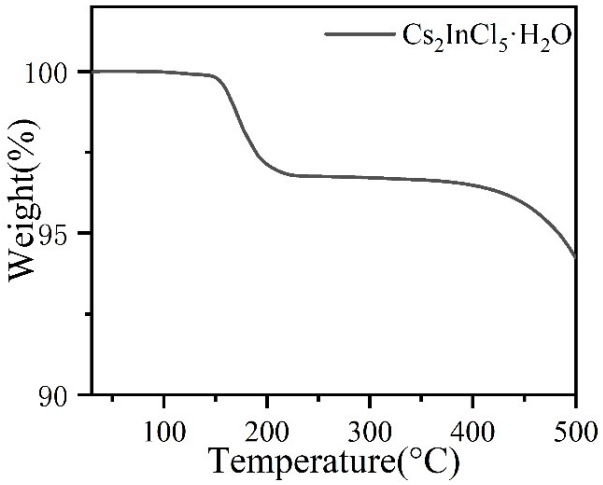

Fig. S9. TG curve of $Cs_2InCl_5 \cdot H_2O$.

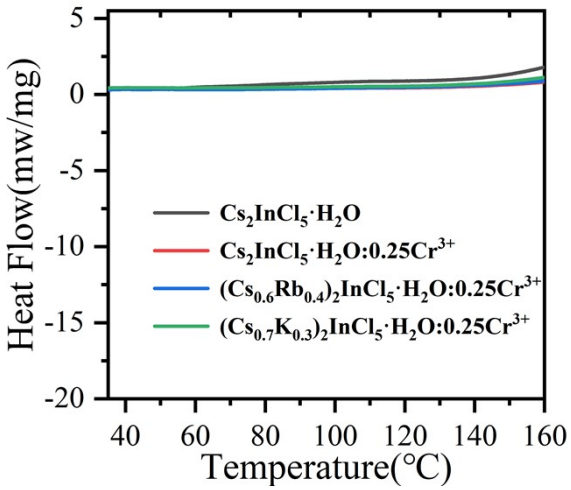

Fig. S10. DSC curves of $Cs_2InCl_5 \cdot H_2O$, $Cs_2InCl_5 \cdot H_2O:0.25Cr^{3+}$, $(Cs_{0.6}Rb_{0.4})_2InCl_5 \cdot H_2O:0.25Cr^{3+}$ and $(Cs_{0.7}K_{0.3})_2InCl_5 \cdot H_2O:0.25Cr^{3+}$.

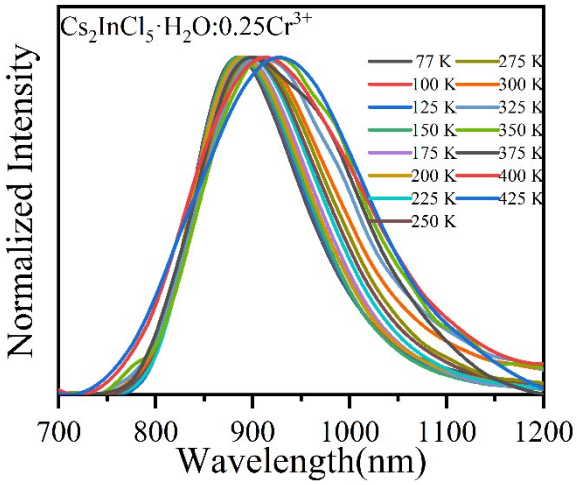

Fig. S11. Normalized temperature-dependent emission spectra of $Cs_2InCl_5 \cdot H_2O$:0.25Cr^{3+} from 77 to 425 K.

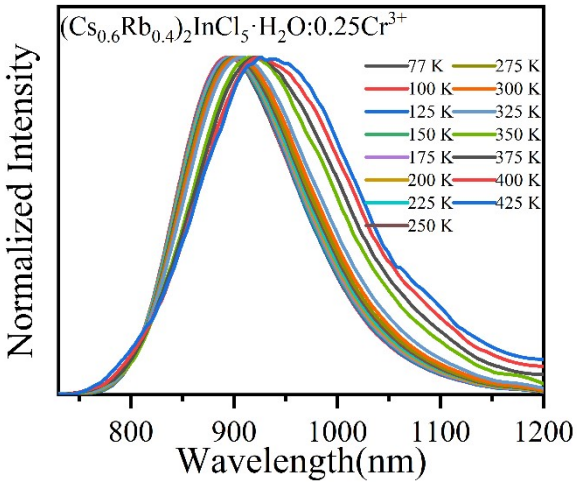

Fig. S12. Normalized temperature-dependent emission spectra of $(Cs_{0.6}Rb_{0.4})_2InCl_5 \cdot H_2O:0.25Cr^{3+}$ from 77 to 425 K.

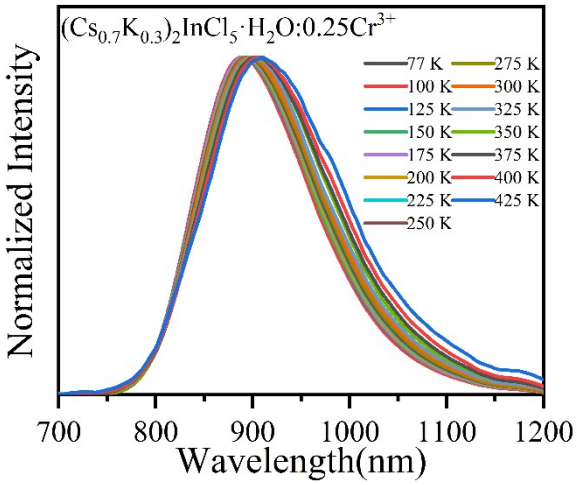

Fig. S13. Normalized temperature-dependent emission spectra of $(Cs_{0.7}K_{0.3})_2InCl_5 \cdot H_2O:0.25Cr^{3+}$ from 77 to 425 K.

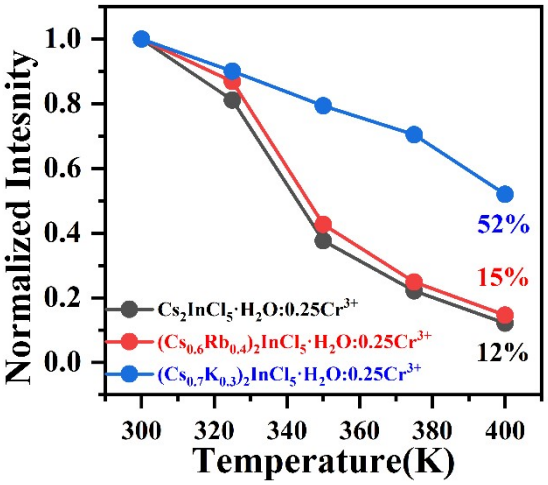

Fig. S14. Temperature-dependent integrated emission intensity of $Cs_2InCl_5{\cdot}H_2O{:}0.25Cr^{3+}$, $(Cs_{0.6}Rb_{0.4})_2InCl_5{\cdot}H_2O{:}0.25Cr^{3+}$ and $(Cs_{0.7}K_{0.3})_2InCl_5{\cdot}H_2O{:}0.25Cr^{3+}$.

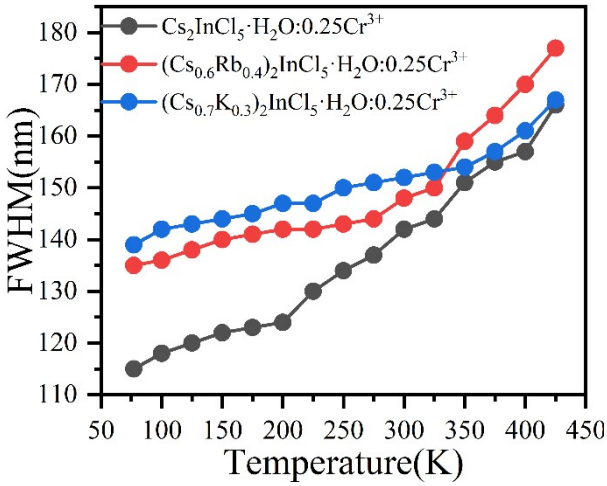

Fig. S15. The dependence of FWHM of the PL spectra for $Cs_2InCl_5·H_2O:0.25Cr^{3+}$, $(Cs_{0.6}Rb_{0.4})_2InCl_5·H_2O:0.25Cr^{3+}$ and $(Cs_{0.7}K_{0.3})_2InCl_5·H_2O:0.25Cr^{3+}$ on temperature.

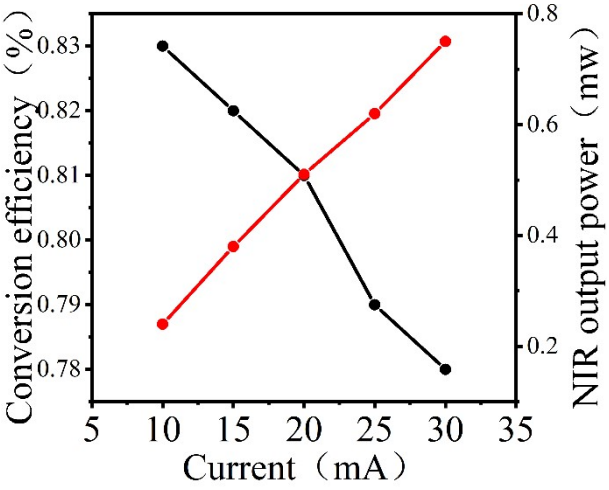

Fig. S16. The output power and photoelectric conversion efficiency of NIR LEDs at different currents.

Table S1. Main parameters of processing and refinement results of $Cs_2InCl_5 \cdot H_2O$ and $Cs_2InCl_5 \cdot H_2O$:0.25Cr^{3+}.

Compound	**$Cs_2InCl_5 \cdot H_2O$**	**$Cs_2InCl_5 \cdot H_2O:Cr^{3+}$**
Space group	Pnma	Pnma
a, Å	14.4167	14.4169
b, Å	10.3843	10.3806
c, Å	7.4117	7.4125
V, $Å^3$	1109.5829	1109.3217
$\alpha = \beta = \gamma$, °	90	90
Uiso(Cr)		0.006
Rwp, %	9.144	9.681
Rp, %	6.971	7.010

Table S2. Main parameters of processing and refinement results of $(Cs_{0.6}Rb_{0.4})_2InCl_5 \cdot H_2O{:}0.25Cr^{3+}$ and $(Cs_{0.7}K_{0.3})_2InCl_5 \cdot H_2O{:}0.25Cr^{3+}$.

Compound	**$(Cs_{0.6}Rb_{0.4})_2InCl_5 \cdot H_2O{:}Cr^{3+}$**	**$(Cs_{0.7}K_{0.3})_2InCl_5 \cdot H_2O{:}Cr^{3+}$**
Space group	*P*nma	*P*nma
a, Å	14.4032	14.3061
b, Å	10.3554	10.2748
c, Å	7.4070	7.3610
V, Å^3	1104.7537	1082.0115
$\alpha = \beta = \gamma$, °	90	90
U_{iso}(Cr)	0.005	0.003
R_{wp}, %	7.861	8.539
R_p, %	5.685	6.356